SCIENTIFIC REPORTS

OPEN

SUBJECT AREAS:

PHASE TRANSITIONS AND CRITICAL PHENOMENA

STRUCTURE OF SOLIDS AND LIQUIDS

Received
26 February 2014

Accepted
28 March 2014

Published
24 April 2014

Correspondence and requests for materials should be addressed to P.Z. (zhang_ping@iapcm.ac.cn) or J.Y. (yan_jun@iapcm.ac.cn)

Ab initio molecular dynamics study of high-pressure melting of beryllium oxide

Dafang Li[1], Ping Zhang[1,2] & Jun Yan[1,2]

[1]LCP, Institute of Applied Physics and Computational Mathematics, Beijing 100088, People's Republic of China, [2]Center for Applied Physics and Technology, Peking University, Beijing 100871, People's Republic of China.

We investigate, through first-principles molecular dynamics simulations, the high-pressure melting of BeO in the range $0 \leq p \leq 100$ GPa. The wurtzite (WZ), zinc blend (ZB), and rocksalt (RS) phases of BeO are considered. It is shown that below 40 GPa, the melting temperature for the WZ phase is higher than that for the ZB and RS phases. When the pressure is beyond 66 GPa, the melting temperature for the RS phase is the highest one, in consistent with the previously reported phase diagram calculated within the quasiharmonic approximation. We find that in the medium pressure range between 40 to 66 GPa, the ZB melting data are very close to those of RS, which results from the fact that the ZB structure first transforms to RS phase before melting. The ZB-RS-liquid phase transitions have been observed directly during the molecular dynamics runs and confirmed using the pair correlation functions analysis. In addition, we propose the melting curve of BeO in the form $T_m = 2696.05\ (1 + P/24.67)^{0.42}$, the zero-pressure value of 2696.05 K falling into the experimental data range of 2693 ~ 2853 K.

Beryllium oxide, BeO, is a unique member of the series of alkaline-earth oxides. Unlike the other members of its class (MgO, CaO, SrO, and BaO) all having the rocksalt structure, BeO crystallizes in the wurtzite structure under ambient conditions, which indicates that Be-O chemical bond is not exclusively ionic but has also some covalent character. It therefore has many anomalous properties, which make it useful in diverse technological applications in ceramics and material industries. For example, thanks to its large direct band gap, it has potential to be used in a variety of nanodevices[1,2]. Besides, as one member of the hardest materials[3], BeO has high thermal conductivity[4], low electrical conductivity[5], and high melting point[6] and hence is a good candidate for use in protective coatings[7] and moderator in nuclear reactors[8]. In particular, the melting point indicates the basic reference points in phase diagrams used in high temperature ceramics. Meanwhile, from the fundamental physics point of view, the study of high-pressure behavior of BeO provides a good understanding of the structural, electronic and dynamic properties and the basic mechanisms that are responsible for these properties.

Motivated by the well-known dielectric theory of Phillips and Van Vechten[9,10], the pressure-induced phase transitions have always been the focus of experimental and theoretical studies. Jephcoat *et al.* did not find any evidence of a phase transition at pressures up to 55 GPa through investigating the Raman spectroscopy of BeO[11], while the static x-ray diffraction experiments also showed no phase transitions until the pressure was increased to 137 GPa[12]. On the theoretical side, there still exists discrepancies in prediction of the transition sequence and transition pressure for BeO. Specifically, two kinds of transition sequences were suggested: wurtzite-zinc blend-rocksalt sequence[13–15] and wurtzite-rocksalt sequence[16–19]. The zinc blende BeO was even reported to be a metastable phase with enthalpy very close to that of the wurtzite phase. It is worth noting that these above-mentioned studies were devoted to material properties at zero temperature, without any thermal effects included. Recently, the description of BeO properties was extended to finite temperatures. Song *et al.*[20] and Zhang *et al.*[21] took into account the effect of lattice vibrations to study the structural stability and phase transformation of BeO based on the mean-field-potential approach. The dispersion relations of BeO were measured by x-ray scattering experiment[22] and predicted by density functional perturbation theory[23]. Wdowik *et al.*[24] and Luo *et al.*[25] calculated the phase diagram and thermal properties of BeO within the quasiharmonic approximation. However, the studied temperature range (<2500 K) was well below the melting temperature at high pressures and the anharmonicity was neglected. It should be noted that the study of high pressure-temperature phase diagram of BeO, especially the high-pressure melting curve, is very important. On the one hand, the melting temperatures of the insulating refractory oxide represent the maximum temperatures for the ceramic to use. On the other hand, the melting curve is an important part of the phase space. For example, the melting curve of MgO, another member of the refractory oxides, has been extensively calculated in a wide pressure range, and thus a full and precise phase diagram was constructed[26–28]. Besides, through investigating the high-pressure melting curves of different phases,

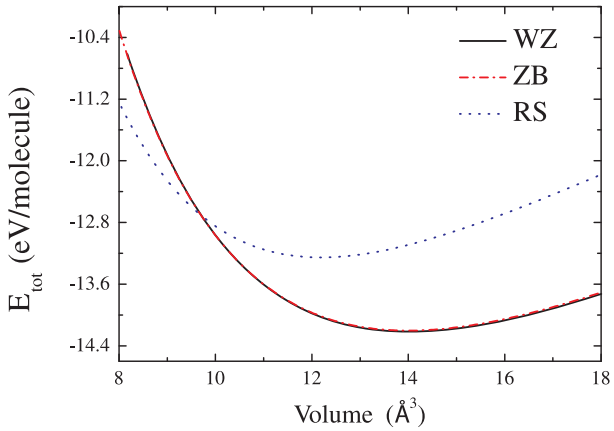

Figure 1 | The total energies for WZ, RS and ZB phase of BeO as a function of BeO molecule volume.

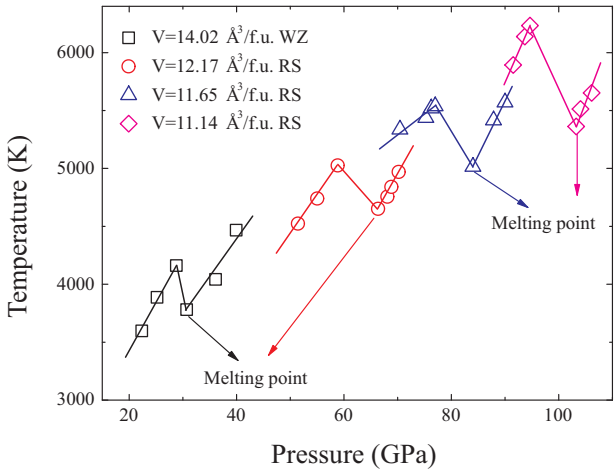

Figure 2 | The Z isochores for volumes 14.02 Å^3/f.u. (WZ), 12.17 Å^3/f.u. (RS), 11.65 Å^3/f.u. (RS) and 11.14 Å^3/f.u. (RS) (shown by the open squares, circles, uptriangles and diamonds correspondingly). The lines are just for eye.

some phase transitions at extreme conditions could be determined, with anharmonicity effects included. Whereas, the studies of BeO at high pressure-temperature conditions are still very scarce and even no theoretical melting data was reported. Therefore, a systematic investigation of BeO melting curve and high pressure-temperature phase transitions is desirable.

In this paper, we calculate the melting curve of BeO up to 100 GPa using the Z-method implemented by first-principles molecular dynamics (FPMD) simulations. Three phases of wurtzite, zinc blend and rocksalt are considered. The interesting ZB-RS-liquid phase transitions are discovered. The analysis of structural change along the isochores suggests an intriguing possibility, that is, the existence of a narrow field of ZB stability separating the WZ and RS phases. The fitted zero-pressure melting temperature is 2696.05 K, in agreement with the experimental value of 2693 to 2853 K[6].

Results

The static DFT calculations at $T = 0$ K for a range of volumes are performed first to assess the performance of our method. The total energies as a function of volume for the WZ, ZB, and RS phases of BeO are presented in figure 1. The lines are obtained from the fit with Murnaghan curve. It can be seen that the energy of the WZ phase is slightly lower than that of the ZB phase, in agreement with the experimental and earlier theoretical results. That is because the WZ and ZB phases have the same local tetrahedral bonding and only differ in the second-nearest neighbors. The minima of the total energy locate at the equilibrium volume (per BeO molecule), which are 14.03 Å^3 (WZ), 13.92 Å^3 (ZB), and 12.17 Å^3 (RS), respectively. We also list the calculated lattice parameters, bulk modulus and elastic constants for the three crystal structures of BeO in Table 1, along with the available experimental and other theoretical data for comparison. In the case of the WZ phase, our calculated lattice constants are higher than the experimental data[29], while the elastic constant is somewhat lower. However, these results are still relatively close to the experimental value. For the ZB and RS phases, our results agree well with the FPLAPW results[21].

We then perform Z-method simulations for twelve isochores of the WZ, ZB and RS BeO. For every volume, a number of temperatures are adopted, ranging from 6000 to 15000 K with the interval of 100 ~ 500 K. Normally, the isochore line consists of two branches: one is the "solid" branch, which ends at the limit of superheating temperature and the other is the "liquid" branch, which starts at the melting temperature. Most of our calculated isochores form the Z-letter shape, four of which displayed in Fig. 2. The corresponding melting points are pointed out by the arrows. However, the isochores of 12.83 Å^3/f.u. and 12.257 Å^3/f.u. for the ZB phase present anomalous behavior, as shown in Fig. 3. The initial kinetic energies K are identified aside each points. These two isochores have the similar characteristics. As K increases, the averaged equilibrium temperature and pressure first increase where the initial ZB solid structure probably remains stable. Then when K is further raised to 11000 K and 11300 K for the isochores of 12.83 Å^3/f.u. (ZB) and 12.257 Å^3/f.u. (ZB) respectively, both of the temperatures and pressures drops. This should be induced by the solid phase transformation, which could be confirmed as a ZB-RS transition by the configurations and pair correlation functions later. The following points with higher K connected by the solid line arrows form the Z curves. That is BeO melts from the new solid structure. The melting points could be easily extracted.

To clarify the structural change in BeO along the isochores of 12.83 Å^3/f.u. (ZB) and 12.257 Å^3/f.u. (ZB), we calculate the pair correlation functions (PCFs), which give the possibility of finding an atom of a given type at a given distance from a reference atom. Because of the similarity of these two isochores, we just take the isochore of 12.257 Å^3/f.u. (ZB) as an example. The PCFs, together with atomic structure

Table 1 | Calculated structural parameters for the WZ, ZB and RS phases of BeO, along with the experimental[29] and theoretical FPLAPW[21] data reported in the literature

Phase	Approach	a	c/a	B_0	C_{11}	C_{12}	C_{13}	C_{33}	C_{44}
WZ	This work	2.711	1.624	207	452	97	72	476	141
	Experiment	2.698	1.622	212	460	125	82	490	145
	FPLAPW	2.712	1.623	203	432	120	87	463	142
ZB	This work	3.826		207	335	143			215
	FPLAPW	3.825		201	342	148			208
RS	This work	3.651		240	306	208			299
	FPLAPW	3.648		231	298	214			294

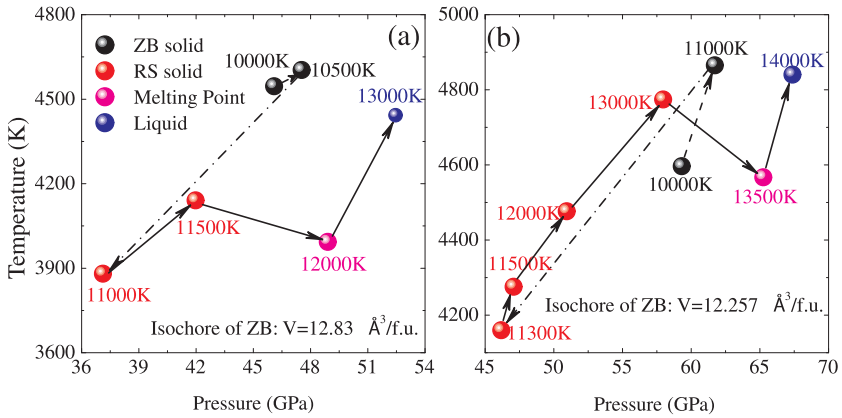

Figure 3 | The isochores of 12.83 Å³/f.u. and 12.257 Å³/f.u. for the ZB phase. The digits aside each points are the corresponding initial kinetic energies.

along the isochore of 12.257 Å³/f.u. (ZB), are presented in Fig. 4. The atomic structure in Fig. 4(a) could be obviously identified as the ZB structure. Further insight into the PCFs, it is concluded that BeO remains in the ZB solid phase for *K* of 10000 K. As *K* increases to 11300 K, both of the atomic structure and PCFs change significantly, but still suggest a solid behavior. For example, the peak structure of g_r(Be-O) at 3 Å for 10000 K disappears as shown in Fig. 4(b). The atom structure and PCFs suggest a RS structure. The PCFs for 13000 K presented in Fig. 4(c) are very similar to those for 11300 K, except the peak values, which demonstrates that ZB-RS transition takes place as *K* is raised to 11300 K and RS structure remains stable for K of 13000 K. Further increase *K* to 13500 K, BeO transforms into a liquid phase, which is indicated in Fig. 4(d) by the complete disordered atomic structure and significant reduction and broadening of maxima of the PCFs, especially for large values of *r*. It should be stressed that these molecular dynamics run in NVE ensemble without any intervention. Therefore, it could be concluded that along the isochores of 12.83 Å³/f.u. (ZB) and 12.257 Å³/f.u. (ZB), BeO first transforms from ZB to RS, and then melts into liquid phase, which is responsible for the anomalous characteristics of the isochores. Though we note that the presented ZB solid points along the isochores in Fig. 3 are in the superheating state, there must exist some points with lower *K* lying in the normal ZB solid state stably. This means ZB solid phase is stable at some lower pressure-temperature conditions, the determination of the specific range depending on the free energy calculations. This conclusion is not totally contrary to the phase transition sequence at zero temperature. As mentioned above, two kinds of zero-temperature transition sequences[13–19] demonstrate that the ZB BeO either doesn't show up or transforms from WZ BeO at high pressures (at least 74 GPa). The presence of lower pressure-temperature ZB BeO should results from the temperature-induced transition from WZ BeO. i.e., the temperature stabilizes the ZB phase over the WZ phase. Here the transition mechanisms can be described in terms of slight modification in the ordering and displacement of Be and O atoms. Though Wdowik *et al.* have pointed out that the ZB structure is energetically not preferred

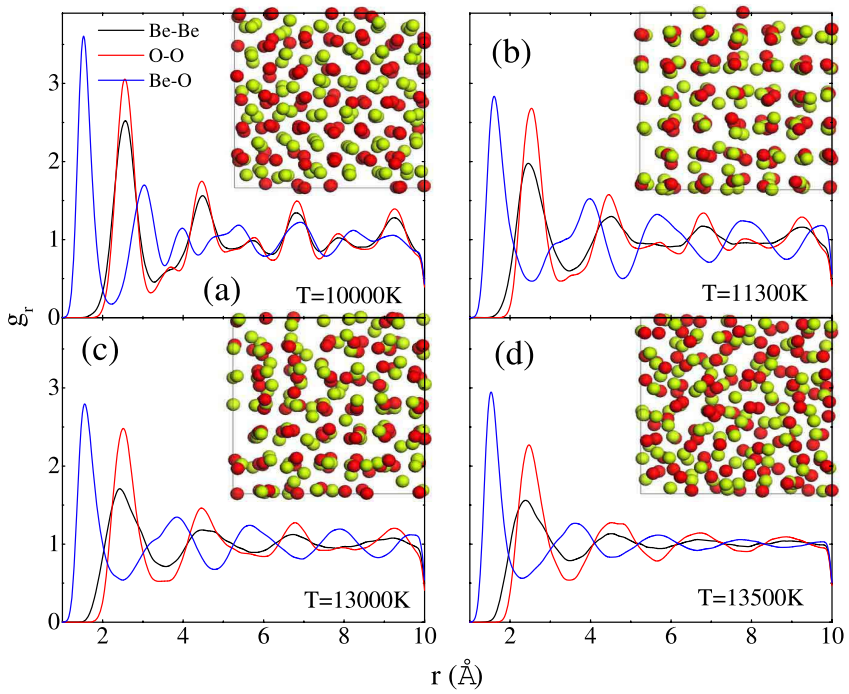

Figure 4 | Pair-correlation functions for Be-Be (black), O-O (red) and Be-O (blue) along the isochore of 12.257 Å³/f.u. for the ZB phase. The atomic structure, where Be and O atoms are denoted by red and green balls, respectively, is also provided in the insets. The corresponding initial kinetic energy is (a) 10000 K; (b) 11300 K; (c) 13000 K; and (d) 13500 K.

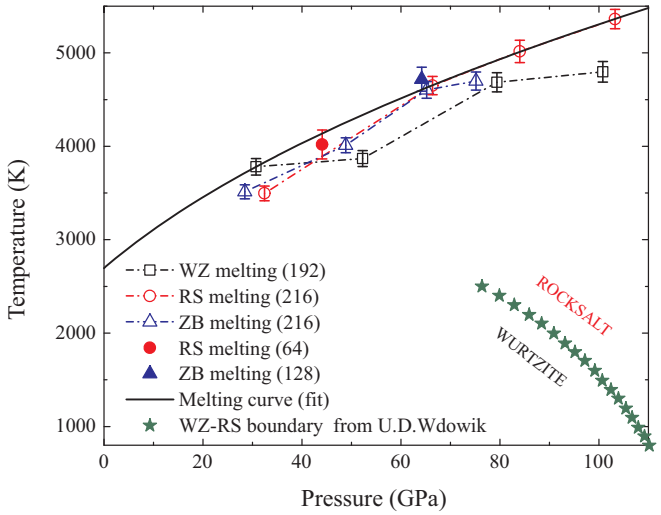

Figure 5 | Melting data of BeO, along with WZ-RS boundary from quasiharmonic approximation. The dash dot line with squares, circles and uptriangles represent the melting conditions for the WZ, RS and ZB phases, respectively. The fitted BeO melting curve is shown as solid thick curve. The stars stand for the WZ-RS boundary in Ref. 24.

below 130 GPa and 2500 K[24], whether it is thermo-dynamically stable in the region depends on accurate free energy calculations or experiments.

The extracted melting points of the WZ, RS and ZB phases are plotted in Fig. 5, along with WZ-RS boundary from Ref. 24. The error bars reflect the standard deviations of the average temperature in our simulations. To our opinion, the largest source of the uncertainty in the calculation of melting point comes from the simulation time not long enough to reach real melting. Size effect turn out to be negligible: the ZB 216-atom and 128-atom results overlap with uncertainties, and the RS 64-atom point lies very close to the 216 atom melting curve, as shown in Fig. 5. It is known that the structure with the higher melting temperature is the more stable phase. Comparison of our WZ, ZB and RS melting points shows that WZ melts at higher temperature below 40 GPa than the other two structure while the melting temperature of RS is the highest above 66 GPa, which means that WZ is stable at low pressures while RS stabilizes at high pressures, in agreement with the quasiharmonic phonon calculations from Wdowik *et al.*[24] qualitatively. In the pressure range between 40 GPa and 66 GPa, the melting temperatures are nearly the same for the RS and ZB phases. Surprisingly, these melting points of ZB just come from the anomalous isochores discussed above. The structural analysis has confirmed that the ZB structure first transforms into the RS phase, and then melts from the RS phase. Therefore, near the melting curve in the medium pressure range, the RS structure is more stable than ZB. Further, we fit our melting data from the isochores of 14.02 Å^3/f.u. (WZ), 12.17 Å^3/f.u. (RS), 11.65 Å^3/f.u. (RS) and 11.14 Å^3/f.u.(RS) using Simon equation, and yields BeO melting curve (P in GPa, and T_m in K)

$$T_m(P) = 2696.05(1 + P/24.67)^{0.42} \quad (1)$$

The predicted zero-pressure melting temperature of 2696.05 K is in agreement with the experimental value of 2693 to 2853 K[6].

Discussion

The high-pressure melting behavior of BeO up to 100 GPa has been studied using the Z-method based on FPMD simulations. We discover that the BeO WZ melting point lies above those of RS and ZB at $P < 40$ GPa, while for pressure above 40 GPa, BeO melts from the RS phase. It's found that in the medium pressure range between 40 to 66 GPa, the ZB melting points are very close to those of RS. That is because before melting, the ZB phase transforms to RS phase first, which has been observed in molecular dynamics process and confirmed by the structural analysis. It is indicated that there probably exist temperature-induced phase transitions of WZ-ZB-RS. These new findings mean that more interesting phenomena and mechanisms remain to be explored in the high temperature-pressure phase diagram of BeO. In addition, our melting curve provides a reference for the technological applications of BeO. Overall, it has high thermal stability with the melting temperatures higher than about 2700 K and thus is indeed a good candidate for use in coatings, nanodevices, catalysts, and moderator in nuclear reactors.

Methods

The main strategy used here to calculate the melting curve follows the Z-method, which is proposed by Belonoshko *et al.*[30]. The idea is to perform FPMD simulations in the microscopic ensemble (NVE) on a single solid system at different initial kinetic energies (K). A realistic limit of superheating can be reached without any external intervention on the dynamics of the melting process. On further increasing K slightly, the temperature will drop naturally to the melting temperature as the latent heat is removed from the kinetic energy. The connected P-T points on the isochore form a characteristic shape similar to the letter Z. The Z method is a good alternative to the two-phase method or the coexistence method because it allows one to derive melting temperatures in close agreement with the two-phase method but with a comparatively modest computational effort. It has been proven successful to predict the melting temperatures in several systems, such as Al[31], H[32], MgO[27], Pt[33], and even the anomalous melting behavior of Li[34]. In addition, a comparably large number of atoms and long runs are still needed to achieve complete melting of the system.

We perform the Z-method simulations of BeO melting with Vienna *ab initio* simulation package (VASP) for WZ (for four volumes, 14.02 Å^3/f.u., 12.68 Å^3/f.u., 11.76 Å^3/f.u. and 11.08 Å^3/f.u., where f.u. denotes a formula unit of BeO), ZB (for four volumes, 14.00 Å^3/f.u., 12.83 Å^3/f.u., 12.257 Å^3/f.u. and 11.89 Å^3/f.u.), and RS (for four volumes, 13.18 Å^3/f.u., 12.17 Å^3/f.u., 11.65 Å^3/f.u. and 11.14 Å^3/f.u.). The calculations are based on density functional theory (DFT) in the finite-temperature formulation due to Mermin. The all-electron projector augmented wave (PAW) method is adopted, with the exchange-correlation potential treated as Perdew-Burke-Ernzerhof (PBE) formalism, as implemented in the VASP code. We fix the plane-wave cut-off at 400 eV. The Brillouin zone is sampled with Γ–point for molecular dynamics. For each density, integration of the equations of motion proceeds with a time step of 0.3–1.0 fs for different pressure-temperature ranges and the energy drift with such a small time step is negligible. In each of the simulations, the time scale lies between 10 and 20 ps. The computational cells are constructed with 196, 216 and 216 atoms for WZ, ZB and RS structure, respectively. Additional convergence tests for the particle number are performed, which includes (i) Z-method melting simulations with 128-atom ZB supercell at 12.257 Å^3/f.u.; (ii) Z-method melting simulations with 64-atoms RS supercell at 13.18 Å^3/f.u.

The zero-temperature energy calculations are performed by means of the linear tetrahedron method with Blöchl's correction[35], while relaxation procedures and force calculations are carried out according to the Methfessel-Paxton scheme[36]. The plane-wave cut-off is fixed at 1250 eV, and the Brillouin zone is sampled using a $15 \times 15 \times 8$ and $16 \times 16 \times 16$ Monkhorst net for integration in the reciprocal space. The total energies are converged to within 0.5 meV/atom.

1. Sorokin, P. B., Fedorov, A. S. & Chernozatonskiĭ, L. A. Structure and properties of BeO nanotubes. *Phys. Solid State* **48**, 398–401 (2006).
2. Baumeier, B., Krüger, P. & Pollmann, J. Structural, elastic, and electronic properties of SiC, BN, and BeO nanotubes. *Phys. Rev. B* **76**, 085407 (2007).
3. Hazen, R. M. & Finger, L. W. High-pressure and high-temperature crystal chemistry of beryllium oxide. *J. Appl. Phys.* **59**, 3728–3733 (1986).
4. Slack, G. A. & Austerman, S. B. Thermal conductivity of BeO single crystals. *J. Appl. Phys.* **42**, 4713–4717 (1971).
5. Roessler, D. M., Walker, W. C. & Loh, E. Electronic spectrum of crystalline beryllium oxide. *J. Phys. Chem. Solids* **30**, 157–167 (1969).
6. Hlaváč, J. Melting temperatures of refractory oxides: Part I. *Pure Appl. Chem.* **54**, 682–688 (1982).
7. Duman, S., Sütlü, A., Bagcl, S., Tütüncü, H. M. & Srivastava, G. P. Structural, elastic, electronic, and phonon properties of zinc-blende and wurtzite BeO. *J. Appl. Phys.* **105**, 033719 (2009).
8. Loh, E. Optical phonons in BeO crystals. *Phys. Rev.* **166**, 673–678 (1968).
9. Phillips, J. C. *Bonds and Bands in Semiconductors*, (*Academic*, New York, 1973).
10. Phillips, J. C. Ionicity of chemical bond in crystals. *Rev. Mod. Phys.* **42**, 317–356 (1970).
11. Jephcoat, A. P., Hemley, R. J., Mao, H. K., Cohen, R. E. & Mehl, M. J. Raman spectroscopy and theoretical modeling of BeO at high pressure. *Phys. Rev. B* **37**, 4727–4734 (1988).
12. Mori, Y., Ikai, T. & Takarabe, K. Photon Factory Activity Report. Part B: *High pressure science* **20**, 215 (2003).

13. Van Camp, P. E. & Van Doren, V. E. Ground-state properties and structural phase transformation of beryllium oxide. *J. Phys. Condens. Matter* **8**, 3385–3390 (1996).
14. Boettger, J. C. & Wills, J. M. Theoretical structural phase stability of BeO to 1 TPa. *Phys. Rev. B* **54**, 8965–8968 (1996).
15. Park, C. J., Lee, S. G., Ko, Y. J. & Chang, K. J. Theoretical study of the structural phase transformation of BeO under pressure. *Phys. Rev. B* **59**, 13501–13504 (1999).
16. Cai, Y., Wu, S., Xu, R. & Yu, J. Pressure-induced phase transition and its atomistic mechanism in BeO: a theoretical calculation. *Phys. Rev. B* **73**, 184104 (2006).
17. Amrani, B., Hassan, F. E. H. & Akbarzadeh, H. First-principles investigations of the ground-state and excited-state properties of BeO polymorphs. *J. Phys. Condens. Matter* **19**, 436216 (2007).
18. Yu, B. R., Yang, J. W., Guo, H. Z., Ji, G. F. & Chen, X. R. Phase transition and elastic properties of BeO under pressure from first-principles calculations. *Physica B* **404**, 1940–1946 (2009).
19. Sahariah, M. B. & Ghosh, S. Dynamical stability and phase transition of BeO under pressure. *J. Appl. Phys.* **107**, 083520 (2010).
20. Song, H. F., Liu, H. F. & Tian, E. Structural and thermodynamic propertis of hexagonal BeO at high pressures and temperatures. *J. Phys. Condens. Matter* **19**, 456209 (2007).
21. Zhang, Q. L., Zhang, P., Song, H. F. & Liu, H. F. Mean-field potential calculations of high-pressure equation of state for BeO. *Chin. Phys. B* **17**, 1341–1348 (2008).
22. Bosak, A., Schmalzl, K., Krisch, M., van Beek, W. & Kolobanov, V. Lattice dynamics of beryllium oxide: inelastic x-ray scattering and ab initio calculations. *Phys. Rev. B* **77**, 224303 (2008).
23. Sahariah, M. B. & Ghosh, S. Ab initio calculation of lattice dynamics in BeO. *J. Phys. Condens. Matter* **20**, 395201 (2008).
24. Wdowik, U. D. Structural stability and thermal properties of BeO from the quasiharmonic approximation. *J. Phys. Condens. Matter* **22**, 045404 (2010).
25. Luo, F., Cheng, Y., Cai, L. C. & Chen, X. R. Structure and thermodynamic properties of BeO: Empirical corrections in the quasiharmonic approximation. *J. Appl. Phys.* **113**, 033517 (2013).
26. Alfé, D. Melting curve of MgO from first-principles simulations. *Phys. Rev. Lett.* **94**, 235701 (2005).
27. Belonoshko, A. B., Arapan, S., Martonak, R. & Rosengren, A. MgO phase diagram from first principles in a wide pressure-temperature range. *Phys. Rev. B* **81**, 054110 (2010).
28. Boates, B. & Bonev, S. A. Demixing instability in dense molten MgSiO3 and the phase diagram of MgO. *Phys. Rev. Lett.* **110**, 135504 (2013).
29. Sirota, N. N., Kuzmina, A. M. & Orlova, N. S. Elastic-moduli of beryllium-oxide at 10–720 K, from the X-ray data. *Dokl. Akad. Nauk SSSR* **314**, 856–862 (1990).
30. Belonoshko, A. B., Skorodumova, N. V., Rosengren, A. & Johansson, B. Melting and critical superheating. *Phys. Rev. B* **73**, 012201 (2006).
31. Bouchet, J., Bottin, F., Jomard, G. & Zérah, G. Melting curve of aluminum up to 300 GPa obtained through ab initio molecular dynamics simulations. *Phys. Rev. B* **80**, 094102 (2009).
32. Davis, S. M., Belonoshko, A. B. & Johansson, B. High-pressure melting curve of hydrogen. *J. Chem. Phys.* **129**, 194508 (2008).
33. Belonoshko, A. B. & Rosengren, A. High-pressure melting curve of platinum from ab initio Z method. *Phys. Rev. B* **85**, 174104 (2012).
34. Li, D. F., Zhang, P., Yan, J. & Liu, H. Y. Melting curve of lithium from quantum molecular-dynamics simulations. *EuroPhys. Lett.* **95**, 56004 (2011).
35. Blöchl, P. E., Jepsen, O. & Andersen, O. K. Improved tetrahedron method for Brillouin-zone integrations. *Phys. Rev. B* **49**, 16223 (1994).
36. Methfessel, M. & Paxton, A. T. High-precision sampling for Brillouin-zone integration in metals. *Phys. Rev. B* **40**, 3616 (1989).

Acknowledgments

This work was supported by National Magnetic Confinement Fusion Science Program of China under Grant 2012GB1066001, NSFC under Grants No. 11205019, No. 11004012 and No. 11275032, by the National Fundamental Security Research Program of China, and by the Foundations for Development of Science and Technology of China Academy of Engineering Physics under Grant No. 2011A0102007 and 2012B0102012.

Author contributions

D.F.L. did the calculations. P.Z., J.Y. and D.F.L. analyzed the results and wrote the paper. P.Z. and J.Y. were responsible for project planning and execution.

Additional information

Competing financial interests: The authors declare no competing financial interests.

How to cite this article: Li, D.F., Zhang, P. & Yan, J. *Ab initio* molecular dynamics study of high-pressure melting of beryllium oxide. *Sci. Rep.* **4**, 4707; DOI:10.1038/srep04707 (2014).